The Addition Effect of CH₃Br on Methane Ignition behind Reflected Shock Waves

Sung Bae Jee, Kilyoung Kim, and Kuan Soo Shin[*]

Department of Chemistry, Soongsil University, Seoul 156-743, Korea
Received May 15, 2000

The addition effect of CH_3Br on the ignition of methane was investigated in the temperature range of 1537-1920 K behind reflected shock waves. The ignition delay times were measured by the sudden increase of pressure and OH emission in the CH_4-O_2-Ar system containing small amount of CH_3Br. The delay times of mixtures with CH_3Br were shorter than those without CH_3Br. The promotion of ignition by CH_3Br was caused by the relative fast decomposition rate in additive. To clarify the addition effect of CH_3Br from the viewpoint of the reaction mechanism, computational analyses were performed in CH_4-CH_3Br-O_2-Ar mixtures.

Introduction

It has been shown that methane has the longest ignition delay time among the simple aliphatic hydrocarbons.[1-6] It was also shown that by adding small amounts of some hydrocarbons or hydrocarbon derivatives to methane, it was possible to shorten and control its ignition delay time.[7] These phenomena were rationalized by the fact that the C-H bond in methane is considerably stronger than the C-C bond in larger hydrocarbons. The initiation due to $CH_4 + M \rightarrow CH_3 + H + M$ in methane is therefore much slower than the equivalent one in other hydrocarbons which proceeds according to R_1-$R_2 \rightarrow R_1 + R_2$ reaction. Whereas it is rather simple to decrease the ignition delay time of methane, it is not known to increase the ignition delay of methane by some additives.

Halogen containing compounds (RX) such as halons are effective and widely used as fire suppressants.[8,9] Westbrook[10] has reported that halogen acid (HX) generated by the decomposition of RX captures H atoms in flame through the reaction of $HX + H \rightarrow H_2 + X$. This reaction is competitive with the reaction of $H + O_2 \rightarrow OH + O$ which is the most important chain branching reaction in combustion. The addition of RX in the flame leads to not only a decrease of the H concentration but also some decrease in the OH and O concentrations.

From the chemical kinetic viewpoint, when CH_3Br is added as an additive, it is a question of competition between the higher initiation rate in CH_3Br compound relative to CH_4 and the tendency of Br atom to combine with hydrogen atoms to produce the inert HBr molecule. The addition effects of CH_3Br on the ignition of methane or ethane have been studied by Takahashi *et al.*[11,12] using shock tube technique. They reported the opposite effect of CH_3Br on methane and ethane ignitions. In their works, CH_3Br acts as a promotor for methane ignition[11] but it acts as an inhibitor for ethane ignition.[12] The differences of predominant reaction in both fuels caused the different effects in methane and ethane ignitions.

In this investigation, the ignition delay times of stoichiometric CH_4-O_2-Ar mixtures in the presence and absence of CH_3Br were measured behind reflected shock waves to examine the effect of CH_3Br and to determine the concentration dependence of CH_3Br on the ignition of methane. Computer analyses were also performed in CH_4-CH_3Br-O_2-Ar mixtures with a model mechanism consisting of 86 reactions to examine the role of bromine for the methane ignition.

Experimental Section

The experiments were done behind reflected shock waves in stainless-steel shock tube which was described in detail elsewhere.[13,14] Therefore, only a brief description of the system, along with a unique to the current experimental procedures, will be presented here. The apparatus consists of a 514 cm (6.02 cm i.d.) 304 stainless-steel tube separated from the He driver chamber by a 0.1 mm thickness unscored aluminium diaphragm. The tube was routinely pumped between experiments to $< 10^{-7}$ torr by turbo molecular pump (Varian, 969-9002) system. The velocity of shock wave was measured with 5 pressure transducers (PCB 113A21) amounted along the end portion of the shock tube, and the temperature and density in the reflected shock wave regime were calculated from this velocity. This procedure has been given previously, and the corrections for boundary-layer perturbation were applied.[15]

Ignition delay time, τ, was defined as the time interval between the arrival of the reflected shock and the onset of an ignition. The pressure measurements were made using a pressure transducer (PCB 113A21) which was located at 1.0 cm from the reflecting surface. The characteristic ultraviolet emission from OH radicals at 306.7 nm was monitored using a photomultiplier tube (ARC DA-781) with a band path filter (Andower, 307 nm) through the sapphire window which was mounted flush at 1.0 cm from the shock tube end plate. The window was masked to 1 mm slit width in order to reduce emission intensity and improve the time resolution of the system. Both traces were fed into a digital oscilloscope (HP45601A). Figure 1 shows the typical oscilloscope trace of the pressure and OH emission profiles. The upper beam records the pressure and the lower beam the OH emission. It was noted that the OH emission traces indicated slightly shorter ignition delay times than the pressure traces. Although this condition prevailed in all mixtures, these dif-
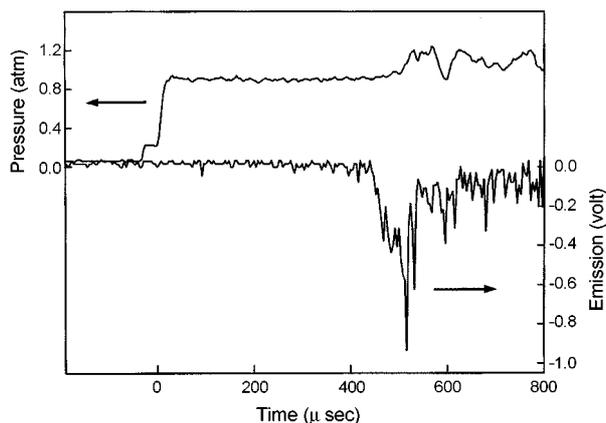
Figure 1. Typical experimental record showing pressure (upper) and OH emission (lower). Experimental conditions were $P_1 = 20.0$ torr and $T_5 = 1586$ K in mixture 2.

Table 1. Experimental condition

|	CH_4 (%)	O_2 (%)	CH_3Br (%)	Ar (%)	T_5 (K)	τ (μs)
Mixture 1	3.5	7.0		89.50	1618-1920	72-1176
Mixture 2	3.5	7.0	0.18	89.32	1537-1808	64-896
Mixture 3	3.5	7.0	0.35	89.15	1545-1761	84-802
Mixture 4	3.68	7.0		89.32	1643-1938	52-1175

ferences were within an accuracy of 5% compared to the total ignition delay time.

The compositions of the mixtures used in this work are given in Table 1. CH_4 (99.99%), CH_3Br (99.5%), O_2 (99.999 %) and Ar (99.999%) were used without further purification. He (99.999%) was used as a driver gas. Four test gas mixtures were prepared manometrically and stored at aluminium cylinders. The initial pressure (P_1) was fixed to 20 torr and the shock velocity could be controlled by changing the pressure of the He driver gas. The measurements covered a temperature range of 1537-1920 K behind reflected shock waves and the measured ignition delay times ranged from 64-1176 μs.

Results and Discussion

In order to examine the role of the bromine additives on methane ignition, the differences between experimental compositions including and excluding bromine atoms must be reduced as much as possible. In mixtures 2, 0.18% of CH_3Br (5% of CH_4) were added and in mixture 3, 0.35% of CH_3Br (10% of CH_4) were added to the reference composition of mixture 1, respectively. The additive, CH_3Br, used in this study is a kind of fuel, so we need to determine how a small additional amount of fuel changes the ignition delay. In mixtures 4, 0.18% more methane was added to the reference composition of mixture 1 to find the role of additional methane on methane ignition.

As shown in Figure 2, ignition delay times of mixture 4 are slightly longer than those of mixture 1; namely, CH_4 acts as a self inhibitive compound. This self inhibitive effect of
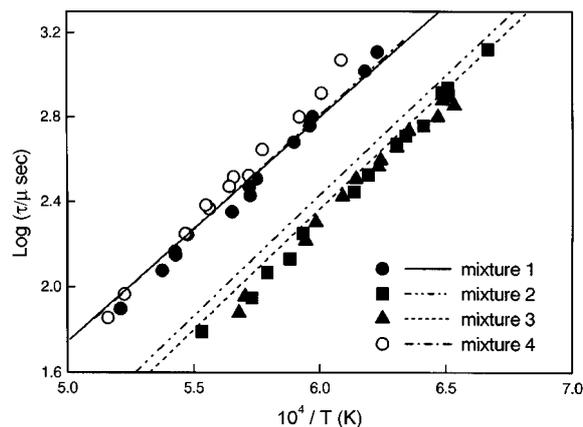
Figure 2. Ignition delay times for the mixtures shown in Table 1. Lines indicate the ignition delays calculated using Table 2 mechanism.

methane in methane ignition can be explained by the competition between the reaction of $H + CH_4 \rightarrow H_2 + CH_3$ and the chain branching reaction of $H + O_2 \rightarrow OH + O$.[13] Figure 2 also shows that ignition delay times of mixtures including CH_3Br are short in comparison with the times for mixture 1. The short ignition delays in mixtures 2 and 3 may be explained qualitatively by only the difference of bond dissociation energies of CH_3-H (453 kJ/mol at 298 K) and CH_3-Br (293 kJ/mol at 298 K).

To clarify the addition effects of CH_3Br on the basis of chemical kinetics, ignition delay times were calculated using detailed reaction mechanism presented in Table 2. The reaction mechanism assembled for methane oxidation consists of 75 elementary reactions (R1-R75 in Table 2) chosen from the GRI-Mech[16] which has been extensively tested and optimized for previous methane combustion studies.[6] To complete the reaction model in presence of CH_3Br, 11 reactions involving Br-containing species (B1-B11 in Table 2) were added to the reaction for methane oxidation. The rate constants for reactions from B1 to B11 were adapted from the NIST database.[17] The reduction techniques using sensitivity and flow analyses[18] were used to choose the final 36 species and 86 elementary reactions to simulate the ignition delay times of CH_4-CH_3Br-O_2-Ar mixtures. The simulations were carried out using Sandia CHEMKIN code.[19] In the simulation, the forward rate constants were used as shown in Table 2 and the reverse rate constants are computed from the forward ones and the appropriate equilibrium constants. The thermodynamic data for the chemical species were taken from the NIST database.[17]

The calculated ignition delay time was defined by the time to reach a sudden increase of OH concentration in the calculation. Figure 2 also shows the comparison between the observed ignition delay times (symbols in Figure 2) and the calculated ones (lines in Figure 2). The calculated ignition delay times are generally in good agreement with the measured ones within the uncertainties of experiments. It is obvious that the reaction mechanism can express the experimental result about the promoting effect of CH_3Br in meth-

Table 2. Reaction Mechanism for CH$_4$-O$_2$-CH$_3$Br-Ar mixtures

Reaction	A	n	E
R1 H + CH$_3$ (+M) = CH$_4$ (+M)	1.782E+16	-0.630	1600.
LOW / 2.477E+33 -4.760 2440./			
TROE / 0.7830 78.00 1995. 5590./			
R2 H + CH$_4$ = CH$_3$ + H$_2$	6.600E+08	1.620	45400.
R3 O + CH$_4$ = OH + CH$_3$	1.020E+09	1.500	36000.
R4 OH + CH$_4$ = CH$_3$ + H$_2$O	1.000E+08	1.600	13100.
R5 CH$_3$ + O$_2$ = O + CH$_3$O	3.083E+13	0.000	120000.
R6 CH$_3$ + O$_2$ = OH + CH$_2$O	3.600E+10	0.000	37400.
R7 CH$_3$ + H$_2$O$_2$ = HO$_2$ + CH$_4$	2.450E+04	2.470	21700.
R8 2CH$_3$ (+M) = C$_2$H$_6$ (+M)	2.120E+16	-0.970	2590.
LOW / 1.770E+50 -9.670 6220./			
TROE / 0.5325 151.00 1038. 4970./			
R9 2CH$_3$ = H + C$_2$H$_5$	4.990E+12	0.100	44400.
R10 CH$_3$ + HCO = CH$_4$ + CO	2.648E+13	0.000	0.
R11 CH$_3$ + CH$_2$O = HCO + CH$_4$	3.320E+03	2.810	24500.
R12 O + CH$_3$ = H + CH$_2$O	8.430E+13	0.000	0.
R13 OH + CH$_3$ = CH$_2^*$ + H$_2$O	2.500E+13	0.000	0.
R14 HO$_2$ + CH$_3$ = O$_2$ + CH$_4$	1.000E+12	0.000	0.
R15 HO$_2$ + CH$_3$ = OH + CH$_3$O	1.333E+13	0.000	0.
R16 CH$_2$ + CH$_3$ = H + C$_2$H$_4$	4.000E+13	0.000	0.
R17 H + CH$_3$O (+M) = CH$_3$OH (+M)	5.000E+13	0.000	0.
LOW / 8.600E+28 -4.000 3025./			
TROE / 0.8902 144.00 2838. 45569./			
R18 H + CH$_3$O = H + CH$_2$OH	3.400E+06	1.600	0.
R19 H + CH$_3$O = H$_2$ + CH$_2$O	2.000E+13	0.000	0.
R20 H + CH$_3$O = OH + CH$_3$	3.200E+13	0.000	0.
R21 H + CH$_3$O = CH$_2^*$ + H$_2$O	1.600E+13	0.000	0.
R22 CH$_3$O + O$_2$ = HO$_2$ + CH$_2$O	4.280E-13	7.600	-14800.
R23 H + CH$_2$O (+M) = CH$_2$OH (+M)	5.400E+11	0.454	15100.
LOW / 1.270E+32 -4.820 6530./			
TROE / 0.7187 103.00 1291. 4160./			
R24 H + CH$_2$O (+M) = CH$_3$O (+M)	5.400E+11	0.454	10900.
LOW / 2.200E+30 -4.800 5560./			
TROE / 0.7580 94.00 1555. 4200./			
R25 H + CH$_2$O = HCO + H$_2$	2.300E+10	1.050	13700.
R26 O$_2$ + CH$_2$O = HO$_2$ + HCO	1.000E+14	0.000	167000.
R27 OH + CH$_2$O = HCO + H$_2$O	3.430E+09	1.180	-1870.
R28 HCO + H$_2$O = H + CO + H$_2$O	3.366E+18	-1.000	71100.
R29 HCO + M = H + CO + M	1.870E+17	-1.000	71100.
R30 HCO + O$_2$ = HO$_2$ + CO	7.600E+12	0.000	1670.
R31 H + O$_2$ + M = HO$_2$ + M	2.800E+18	-0.860	0.
R32 H + 2O$_2$ = HO$_2$ + O$_2$	3.000E+20	-1.720	0.
R33 H + O$_2$ + H$_2$O = HO$_2$ + H$_2$O	1.652E+19	-0.760	0.
R34 H + O$_2$ + N$_2$ = HO$_2$ + N$_2$	3.750E+20	1.720	0.
R35 H + O$_2$ + Ar = HO$_2$ + Ar	7.000E+17	-0.800	0.
R36 H + O$_2$ = O + OH	8.300E+13	0.000	60300.
R37 2H + M = H$_2$ + M	1.000E+18	-1.000	0.
R38 2H + H$_2$ = 2H$_2$	9.000E+16	-0.600	0.
R39 2H + H$_2$O = H$_2$ + H$_2$O	6.000E+19	-1.250	0.
R40 2H + CO$_2$ = H$_2$ + CO$_2$	5.500E+20	-2.000	0.
R41 H + OH + M = H$_2$O + M	2.200E+22	-2.000	0.
R42 H + HO$_2$ = O + H$_2$O	3.970E+12	0.000	2810.
R43 H + HO$_2$ = 2OH	1.340E+14	0.000	2660.
R44 H + CH$_2$OH (+M) = CH$_3$OH (+M)	1.800E+13	0.000	0.
LOW / 3.000E+31 -4.800 3300./			
TROE / 0.7679 338.00 1812. 5081./			
R45 H + CH$_2$OH = H$_2$ + CH$_2$O	2.000E+13	0.000	0.
R46 H + CH$_2$OH = OH + CH$_3$	1.200E+13	0.000	0.

Table 2. Continued

Reaction	A	n	E
R47 H + CH$_2$OH = CH$_2^*$ + H$_2$O	6.000E+12	0.000	0.
R48 H + CH$_3$OH = CH$_2$OH + H$_2$	1.700E+07	2.100	20400.
R49 H + CH$_3$OH = CH$_3$O + H$_2$	4.200E+06	2.100	20400.
R50 H + C$_2$H (+M) = C$_2$H$_2$ (+M)	1.000E+17	-1.000	0.
LOW / 3.750E+33 -4.800 1900./			
TROE / 0.6464 132.00 1315. 5566./			
R51 H + C$_2$H$_2$ (+M) = C$_2$H$_3$ (+M)	5.600E+12	0.000	10000.
LOW / 3.800E+40 -7.270 7220./			
TROE / 0.7507 98.50 1302. 4167./			
R52 H + C$_2$H$_3$ (+M) = C$_2$H$_4$ (+M)	6.080E+12	0.270	1170.
LOW / 1.400E+30 -3.860 3320./			
TROE / 0.7820 207.50 2663. 6095./			
R53 H + C$_2$H$_3$ = H$_2$ + C$_2$H$_2$	3.000E+13	0.000	0.
R54 H + C$_2$H$_4$ (+M) = C$_2$H$_5$ (+M)	1.080E+12	0.454	7620.
LOW / 1.200E+42 -7.620 6970./			
TROE / 0.9753 210.00 984. 4374./			
R55 H + C$_2$H$_6$ = C$_2$H$_5$ + H$_2$	1.150E+08	1.900	31500.
R56 O + H$_2$ = H + OH	5.000E+04	2.670	26300.
R57 O + HO$_2$ = OH + O$_2$	2.000E+13	0.000	0.
R58 O + C$_2$H$_4$ = CH$_3$ + HCO	1.920E+07	1.830	920.
R59 OH + H$_2$ = H + H$_2$O	2.160E+08	1.510	14400.
R60 2OH (+M) = H$_2$O$_2$ (+M)	7.400E+13	-0.370	0.
LOW / 2.300E+18 -0.900 -1700./			
TROE / 0.7349 94.00 1756. 5182./			
R61 OH + HO$_2$ = O$_2$ + H$_2$O	4.616E+13	0.000	-2090.
R62 OH + H$_2$O$_2$ = HO$_2$ + H$_2$O	1.750E+12	0.000	1340.
R63 OH + C$_2$H$_4$ = C$_2$H$_3$ + H$_2$O	3.600E+06	2.000	10500.
R64 CH$_2$ + O$_2$ = OH + HCO	1.320E+13	0.000	6280.
R65 CH$_2$ + H$_2$ = H + CH$_3$	5.000E+05	2.000	30300.
R66 2CH$_2$ = H$_2$ + C$_2$H$_2$	3.200E+13	0.000	0.
R67 CH$_2^*$ + Ar = CH$_2$ + Ar	9.000E+12	0.000	2510.
R68 CH$_2^*$ + O$_2$ = H + OH + CO	2.800E+13	0.000	0.
R69 CH$_2^*$ + O$_2$ = CO + H$_2$O	1.200E+13	0.000	0.
R70 CH$_2$OH + O$_2$ = HO$_2$ + CH$_2$O	1.800E+13	0.000	3770.
R71 C$_2$H$_3$ + O$_2$ = HCO + CH$_2$O	3.980E+12	0.000	-1000.
R72 C$_2$H$_4$ (+M) = H$_2$ + C$_2$H$_2$ (+M)	8.000E+12	0.440	371000.
LOW / 7.000E+50 -9.310 99860./			
TROE / 0.7345 180.00 1035. 5417./			
R73 C$_2$H$_5$ + O$_2$ = HO$_2$ + C$_2$H$_4$	8.400E+11	0.000	16200.
R74 HCCO + O$_2$ = OH + 2CO	1.600E+12	0.000	3570.
R75 2HCCO = 2CO + C$_2$H$_2$	1.000E+13	0.000	0.
B1 CH$_3$Br = CH$_3$ + Br	1.580E+13	0.000	300000.
B2 CH$_3$Br + H = CH$_3$ + HBr	5.110E+13	0.000	24400.
B3 CH$_3$Br + Br = CH$_2$Br + HBr	1.000E+14	0.000	68200.
B4 Br + HO$_2$ = HBr + O$_2$	8.430E+12	0.000	4900.
B5 CH$_2$O + Br = HCO + HBr	1.020E+13	0.000	6690.
B6 HBr + H = Br + H$_2$	1.260E+10	1.050	669.
B7 CH$_3$ + HBr = CH$_4$ + Br	9.460E+11	0.000	-1590.
B8 C$_2$H$_5$ + HBr = C$_2$H$_6$ + Br	1.020E+12	0.000	-4180.
B9 CH$_2$OH + HBr = CH$_3$OH + Br	5.240E+11	0.000	-3680.
B10 CH$_2$Br + CH$_3$ = C$_2$H$_4$ + HBr	5.400E+12	0.000	5860.
B11 CH$_2$Br + CH$_3$ = C$_2$H$_5$ + Br	1.000E+13	0.000 .	29300

Rate constants are in the form A x T^n exp(-Ea/RT), in cm^3, mol, s, J, and K. The (+M) indicates that the reaction is a pressure-dependent reaction. For reactions R1, R8, R17, R23, R24, R44, R50, R51, R52, R54, R60, and R72, the tabulated parameters refer to the high pressure limit rate coefficients; three parameters in LOW are the low pressure limit rate coefficients; four parameters in TROE are the falloff parameters that define the temperature dependence of the broadening factor.[20]

1018   *Bull. Korean Chem. Soc.* **2000**, Vol. 21, No. 10

Sung Bae Jee et al.
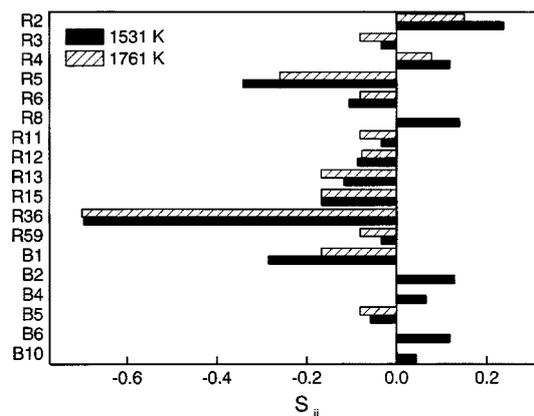
Figure 3. Logarithmic sensitivity spectra[18] of the ignition delay time for mixture 3 with $P_1 = 20.0$ torr. The filled (1531 K) and striped (1761 K) bars were computed by multiplying the Table 2 rate coefficient value by 2. Sensitivities less than 0.05 are not shown.
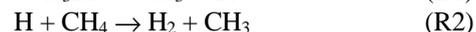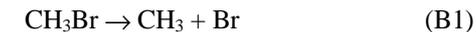
ane ignition.

In the reaction mechanism, not all the elementary reactions contribute equally to the ignition delay times or chemical history. On the contrary, some of them contribute significantly, some marginally, and some not at all. In order to find the sensitive reactions to the ignition delay time, logarithmic sensitivity analysis[18] defined by the following equation was carried out by multiplying the reference rate constants from Table 2 by a factor of 2.

$$S_{ij} = \frac{\Delta \log \tau_i}{\Delta \log k_j}$$

where τ_i is the ignition delay time at condition i and k_j means the rate constant of jth elementary reaction. As shown in Figure 3, the sensitive reactions in CH_4-CH_3Br-O_2-Ar mixtures are the following reactions.

$$H + O_2 \rightarrow OH + O \qquad \text{(R36)}$$
$$CH_3 + O_2 \rightarrow CH_3O + O \qquad \text{(R5)}$$
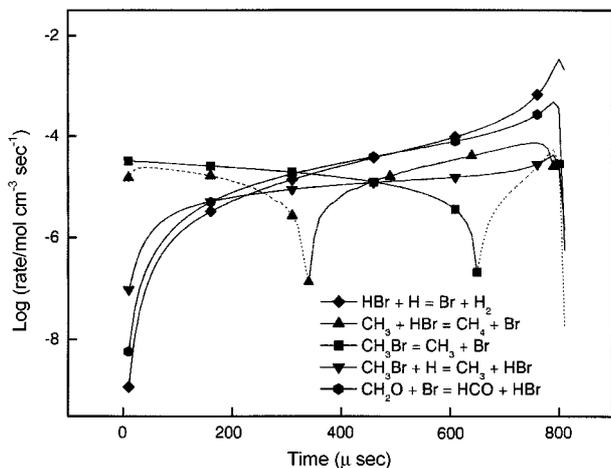
Figure 4. Net reaction rate for mixture 3 at $P_1 = 20.0$ torr and $T_5 = 1531$ K. The solid lines indicate that the net reaction proceeds in the forward direction; the dotted lines indicate the reverse direction.

$$CH_3Br \rightarrow CH_3 + Br \qquad \text{(B1)}$$
$$H + CH_4 \rightarrow H_2 + CH_3 \qquad \text{(R2)}$$

Not only the CH_3Br decomposition reaction (B1) but also the chain branching reaction (R36) and other reactions involving CH_3-radical (R5, R2) are sensitive in the ignition step of CH_4-CH_3Br-O_2-Ar mixtures.

Flow analysis[18] was also carried out by means of the computing net reaction rate defined by the following equation in such a case of reaction for $A + B \rightarrow C + D$.

$$Rate(t) = k_f [A]_t [B]_t - k_r [C]_t [D]_t$$

where k_f and k_r are the forward and reverse rate constants, respectively. $[X]_t$ is the concentration of X species at time t. Figure 4 shows net reaction rates of the important reactions involving Br-species. In the early time of the ignition step, the most important initiation reaction is CH_3Br decomposition reaction (B1). While CH_3 is consumed through $CH_3 + O_2 \rightarrow CH_3O + O$ reaction (R5) which is the main reaction of CH_3 consumption, Br atom consumes CH_4 through the reaction of $Br + CH_4 \rightarrow HBr + CH_3$ (B7). Once HBr is formed, HBr reacts with H to produce H_2 and Br (B6). This reaction (B6) is considered to be the most important retarding step in flame propagation, but it becomes important at the late stage of the combustion process as shown in Figure 4.

The experimental results of this study for the addition effect of CH_3Br on methane ignition are in good agreement with the results of Takahashi *et al.*[11] In their investigation, they reported CH_3Br was regenerated through the reaction of $HBr + CH_3 \rightarrow CH_3Br + H$ (reverse reaction of B2) and proposed closed-loop reactions as shown in Figure 5. The total reaction of their loop is $CH_4 \rightarrow CH_3 + H$ and CH_3Br acts as a catalysis in their loop. However, our simulation shows that B2 reaction proceeds forward direction ($CH_3Br + H \rightarrow HBr + CH_3$) and has small net reaction rate, so CH_3Br could not be regenerated during the whole ignition delay period. The difference of net reaction rate depends on the rate constant of B2. The rate constant for B2 adapted by Takahashi *et al.*[11] was about three times higher than the one used in this study.[17]

In conclusion, the promotion effect by addition of CH_3Br to methane is because of the relative fast decomposition rate in additive, which leads to easy generation of CH_3 radical.
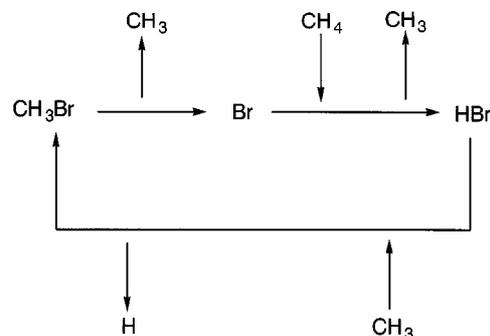
Figure 5. Closed-loop reactions proposed by Takahashi *et al.*[11] See the discussion in the text.

The concentration dependence of CH_3Br on the ignition of methane, however, is small. The modeling investigation of the reaction mechanism (Table 2) gave calculated ignition delay times in good agreement with the experiments.

References

1. Bowman, C. T. *Comb. Sci. Technol*. **1970**, *2*, 161.
2. Lifshitz, A.; Scheller, K.; Burcat, A.; Skinner, G. B. *Combust. Flame* **1971**, *16*, 311.
3. Crossley, R. W.; Dorko, E. A.; Scheller, K.; Burcat, A. *Combust. Flame* **1972**, *19*, 373.
4. Skinner, G. B.; Lifshitz, A.; Scheller, K.; Burcat, A. *J. Chem. Phys.* **1972**, *56*, 3853.
5. Cook, D. F.; Willams, A. *Combust. Flame* **1975**, *24*, 245.
6. Yang, H.; Qin, Z.; Lissianski, V.; Gardiner, W. C. *Israel Journal of Chemistry* **1996**, *36*, 305.
7. Burcat, A. *Combust. Flame* **1975**, *24*, 319.
8. Miziolek, A. W.; Tsang, W. *Halon Replacements Technology and Science*; ACS Symposium Series 611: Washington, D. C., 1995.
9. Leylegian, J. C.; Zhu, D. L.; Law, C. K.; Wang, H. *Combust. Flame* **1998**, *114*, 285.
10. Westbrook, C. K. *Combust. Sci. Technol.* **1983**, *34*, 201.
11. Takayashi, K.; Inomata, T.; Moriwaki, T.; Okazaki. S. *Bull. Chem. Soc. Jpn*. **1988**, *61*, 3307.
12. Takayashi, K.; Inomata, T.; Moriwaki, T.; Okazaki. S. *Bull. Chem. Soc. Jpn*. **1989**, *62*, 2138.
13. Jee, S. B.; Kim, W. K.; Shin, K. S. *J. Korean Chem. Soc.* **1999**, *43*, 156.
14. Baeck, H. J.; Shin, K. S.; Yang, H.; Lissianski, V. V.; Gardiner, W. C. *Bull. Korean Chem. Soc*. **1995**, *16*, 543.
15. Kim, W. K.; Shin, K. S. *J. Korean Chem. Soc.* **1997**, *41*, 600.
16. Frenklach, M.; Wang, H.; Goldenberg, M.; Smith, G. P.; Golden, D. M.; Bowman, C. T.; Hanson, R. K.; Gardiner, W. C., Jr.; Lissianski, V. V. *GRI-Mech; An Optimized Detailed Chemical Reaction Mechanism for Methane Combustion*; Gas Research Institute Topical Report GRI-95/0058: http://www.me.berkeley.edu/gri_mech/ 1995.
17. Mallard, W. G.; Westley, F.; Herron, J. T.; Hampson, R. F.; Frizzel, D. H. NIST *Chemical Kinetics Database, Version 5.0*: NIST, Gaithersburg, U. S. A., 1993.
18. Gardiner, W. C., Jr. *J. Phys. Chem*. **1977**, *81*, 2367.
19. Kee, R. J.; Rupley, F. M.; Meeks, E.; Miller, J. A. *Chemkin-III; A Fortran* Chemical Kinetics Package for the Analysis of Gas-Phase Chemical and Plasma *Kinetics*; Sandia National Laboratories Report SAND96-8216, 1996.
20. Gilber, R. G.; Luther, K.; Troe, J. *Ber. Bunsenges. Phys. Chem.* **1983**, *87*, 169.